

1 Persistent SARS-CoV-2 infection and increasing viral variants in children and young  
2 adults with impaired humoral immunity  
3 Thao T. Truong, PhD<sup>1</sup>, Alex Ryutov, PhD<sup>1</sup>, Utsav Pandey, PhD<sup>2</sup>, Rebecca Yee, PhD<sup>1</sup>,  
4 Lior Goldberg, MD, MSc<sup>3,4</sup>, Deepa Bhojwani, MD<sup>3,4</sup>, Paibel Aguayo-Hiraldo, MD<sup>3,4,9</sup>,  
5 Benjamin A. Pinsky, MD, PhD<sup>5,6</sup>, Andrew Pekosz, PhD<sup>7</sup>, Lishuang Shen, PhD<sup>1</sup>, Scott D.  
6 Boyd, MD, PhD<sup>5,10</sup>, Oliver F. Wirz, PhD<sup>5</sup>, Katharina Röltgen, PhD<sup>5</sup>, Moiz Bootwalla,  
7 MS<sup>1</sup>, Dennis T. Maglinte, MS<sup>1</sup>, Dejerianne Ostrow, PhD<sup>1</sup>, David Ruble, BS<sup>1</sup>, Jennifer H.  
8 Han, MS<sup>1</sup>, Jaclyn A. Biegel, PhD<sup>1,4</sup>, Maggie Li, ScM<sup>7</sup>, ChunHong Huang, MD<sup>5</sup>, Mayala  
9 K. Sahoo, PhD<sup>5</sup>, Pia S. Pannaraj, MD, MPH<sup>4,8</sup>, Maurice O’Gorman, PhD<sup>1,4</sup>, Alexander  
10 R. Judkins, MD<sup>1,4</sup>, Xiaowu Gai, PhD<sup>1,4</sup>, Jennifer Dien Bard, PhD<sup>1,4#</sup>

11

12 <sup>1</sup>Department of Pathology and Laboratory Medicine, Children’s Hospital Los Angeles,  
13 Los Angeles, CA

14 <sup>2</sup>Department of Pathology, Westchester Medical Center/New York Medical College,  
15 Valhalla, NY

16 <sup>3</sup>Department of Pediatrics, Cancer and Blood Disease Institute, Division of Hematology-  
17 Oncology, Children’s Hospital Los Angeles, Los Angeles, CA

18 <sup>4</sup>Keck School of Medicine, University of Southern California, Los Angeles, CA

19 <sup>5</sup>Department of Pathology, Stanford University School of Medicine, Stanford, CA

20 <sup>6</sup>Division of Infectious Diseases and Geographic Medicine, Department of Medicine,  
21 Stanford University School of Medicine, Stanford, CA

22 <sup>7</sup>W. Harry Feinstone Department of Molecular Microbiology and Immunology, Johns  
23 Hopkins Bloomberg School of Public Health, Baltimore, MD

24 <sup>8</sup>Department of Pediatrics, Division of Infectious Diseases, Children’s Hospital Los  
25 Angeles, Los Angeles, CA

26 <sup>9</sup>Department of Pediatrics, Cancer and Blood Disorder Institute, Transplant and Cellular  
27 Therapy Section, Children’s Hospital Los Angeles, CA

28 <sup>10</sup>Sean N. Parker Center for Allergy and Asthma Research, Stanford, CA

29

30 #Address correspondence to Jennifer Dien Bard, [jdienbard@chla.usc.edu](mailto:jdienbard@chla.usc.edu)

31

## 32 **Summary**

### 33 *Background*

34 There is increasing concern that persistent infection of SARS-CoV-2 within  
35 immunocompromised hosts could serve as a reservoir for mutation accumulation and  
36 subsequent emergence of novel strains with the potential to evade immune responses.

### 37 *Methods*

38 We describe three patients with acute lymphoblastic leukemia who were persistently  
39 positive for SARS-CoV-2 by real-time polymerase chain reaction. Viral viability from  
40 longitudinally-collected specimens was assessed. Whole-genome sequencing and  
41 serological studies were performed to measure viral evolution and evidence of immune  
42 escape.

### 43 *Findings*

44 We found compelling evidence of ongoing replication and infectivity for up to 162 days  
45 from initial positive by subgenomic RNA, single-stranded RNA, and viral culture

46 analysis. Our results reveal a broad spectrum of infectivity, host immune responses,  
47 and accumulation of mutations, some with the potential for immune escape.

#### 48 *Interpretation*

49 Our results highlight the need to reassess infection control precautions in the  
50 management and care of immunocompromised patients. Routine surveillance of  
51 mutations and evaluation of their potential impact on viral transmission and immune  
52 escape should be considered.

#### 53 *Funding*

54 The work was partially funded by The Saban Research Institute at Children's Hospital  
55 Los Angeles intramural support for COVID-19 Directed Research (X.G. and J.D.B.), the  
56 Johns Hopkins Center of Excellence in Influenza Research and Surveillance  
57 HHSN272201400007C (A.P.), NIH/NIAID R01AI127877 (S.D.B.), NIH/NIAID  
58 R01AI130398 (S.D.B.), NIH 1U54CA260517 (S.D.B.), an endowment to S.D.B. from the  
59 Crown Family Foundation, an Early Postdoc.Mobility Fellowship Stipend to O.F.W. from  
60 the Swiss National Science Foundation (SNSF), and a Coulter COVID-19 Rapid  
61 Response Award to S.D.B. L.G. is a SHARE Research Fellow in Pediatric Hematology-  
62 Oncology.

63

#### 64 **Introduction**

65 Infection with severe acute respiratory syndrome coronavirus-2 (SARS-CoV-2), the  
66 cause of coronavirus disease 2019 (COVID-19) is most commonly detected using real-  
67 time polymerase chain reaction (RT-PCR). Viral load typically peaks with onset of  
68 symptoms and wanes to undetectable levels by week three, when patients generally

69 begin to develop antibodies.<sup>1</sup> While the Centers for Disease Control and Prevention  
70 (CDC) recommends quarantining for 14 days following exposure to COVID-19, the time  
71 course of infection may vary due to factors including age, immune status, and disease  
72 severity.<sup>2</sup> In most patients, culture, contact tracing, and subgenomic RNA detection  
73 studies have not demonstrated infectivity beyond 10 days of symptom onset.<sup>3,4</sup> In rare  
74 cases prolonged shedding of SARS-CoV-2 has been observed in immunocompromised  
75 adults, making study of this population critically important.<sup>5-8</sup> However, the temporal  
76 dynamics of SARS-CoV-2 infectivity and the evolution of SARS-CoV-2 mutational  
77 profiles over prolonged periods of infection in immunocompromised patients, particularly  
78 in children, have not been described. Beyond the implications for individual patients, the  
79 emergence of B.1.1.7 SARS-CoV-2 and other lineages with potential for immune  
80 evasion has led to greater focus on the importance of genomic surveillance.<sup>9,10</sup> Here,  
81 we describe prolonged SARS-CoV-2 RT-PCR positivity in two children and one young  
82 adult undergoing therapy for B-cell acute lymphoblastic leukemia (ALL). In addition to  
83 evidence of ongoing replication, two of these cases demonstrated significant intra-host  
84 SARS-CoV-2 mutational accumulation and host immune responses that may have  
85 contributed to their disease course.

86

## 87 **Methods**

### 88 **Case histories**

89 Patient 1 is a previously healthy female under 5 years of age with no significant past  
90 medical history prior to several admissions to the emergency department (ED) for  
91 worsening pancytopenia, decreased appetite, and abdominal pain. Her bone marrow

92 biopsy revealed 58% blasts consistent with B-cell ALL and a chemotherapy regimen  
93 was initiated (Figure 1A, Table 1). Asymptomatic screening for SARS-CoV-2 by RT-  
94 PCR at time of discharge revealed a positive result (day 0). She was re-admitted to the  
95 hospital on day 3 for fatigue and vomiting as well as cough, malaise, and  
96 gastrointestinal symptoms and discharged on day 6. She consistently tested positive for  
97 SARS-CoV-2 during follow-up screens for her chemotherapy until she finally tested  
98 negative on day 91 without any notable respiratory symptoms (Figure 1A, Figure 2A).  
99

100 Patient 2 is a male in the 20-25 year age range who was previously diagnosed with B-  
101 cell ALL six months prior to his first SARS-CoV-2 positive RT-PCR. He received  
102 combination chemotherapy, however continued to have detectable residual disease at  
103 the end of the consolidation phase, prompting initiation of CD19-directed chimeric  
104 antigen receptor T cell therapy (CAR-T, Tisagenlecleucel, Cassiopeia protocol). Upon a  
105 follow up visit to the transplant and cell therapy clinic 3 weeks later, the patient was  
106 tested for SARS-CoV-2 due to concerns for possible contact exposure and was positive  
107 (day 0). On day 6 after the initial positive test he presented to the ED with decreased  
108 appetite, fever, and two days of dry cough. His chest x-ray showed a diffuse interstitial  
109 prominence and a small bilateral pleural effusion. He developed intermittent fevers with  
110 increased oxygen requirement over the next several days, including an episode of acute  
111 hypoxemic respiratory failure necessitating 10 liters of oxygen via face mask on day 18.  
112 He received a 5-day course of Remdesivir. From then on his oxygen requirement was  
113 weaned down to 2-3 liters via nasal cannula (NC), however he continued to have  
114 intermittent fevers and bilateral patchy ground glass opacities on chest CT. He

115 improved after a second 5-day course of Remdesivir, weaned down off supplemental  
116 O<sub>2</sub> to his nighttime baseline of 0.5L/NC while asleep (used to treat his mild obstructive  
117 sleep apnea) and was discharged on day 45. He was hospitalized four additional times  
118 for persistent fevers with negative infectious work-up except for a persistently positive  
119 SARS-CoV-2 RT-PCR with consistently high (Ct range: 17.2 – 28.1) viral loads. Weekly  
120 convalescent plasma therapy was initiated on day 103 and changed to biweekly  
121 beginning day 144. Unfortunately on day 156, he developed worsening cough, new  
122 fevers, and was found to be hypoxemic down to 80% needing supplemental oxygen  
123 with 4L/NC. Full infectious disease workup failed to demonstrate any additional infection  
124 besides persistently positive SARS-CoV-2 RT-PCR. He was admitted to the hospital  
125 and received convalescent plasma. Thereafter, he resumed weekly convalescent  
126 plasma infusions. His anti-SARS-CoV-2 IgG was finally positive on day 103 which was  
127 likely due to the plasma infusion. He has remained SARS-CoV-2 RT-PCR positive  
128 through his most recent test on day 250 at the time of this publication.

129

130 Patient 3 is a male under 5 years of age who was diagnosed with high-risk B-cell ALL 7  
131 months prior to presentation to the ED with fever and confirmed positive for SARS-CoV-  
132 2 upon admission (day 0). At admission he demonstrated tachycardia and pancytopenia  
133 that were attributed to his chemotherapy. After clinical improvement, he was discharged  
134 on day 6 but re-admitted on day 14 with recurrent fever and tachycardia. He continued  
135 to be febrile, had worsening pancytopenia, pulmonary infiltrates, and increasing oxygen  
136 requirements to 5L via face mask by day 32, at which time he received a 5-day regimen  
137 of Remdesivir. His fevers and respiratory distress improved and he was discharged on

138 day 40, only to be readmitted for fever on day 43 and discharged on day 51. The patient  
139 then started maintenance chemotherapy. Anti-SARS-CoV-2 IgG was repeatedly  
140 negative or borderline and finally became positive on day 83. He was re-admitted on  
141 day 162 for possible urinary tract infection and subsequently developed tachypnea,  
142 fever, and cytopenia. Chest CT scans on days 47, 96, and 166 showed persistent  
143 multifocal pneumonia and scattered areas of ground-glass and consolidative opacities,  
144 with shifting opacities that increased in some areas but improved in others. He improved  
145 on antibiotics and was discharged on resolution of his fevers on day 173. He was last  
146 RT-PCR positive on day 162 and finally negative on day 196. A surveillance chest CT  
147 scan on day 230 showed near complete resolution of his pulmonary disease.

148

#### 149 **Study cohort**

150 Specimens from all three patients were obtained at Children's Hospital Los Angeles  
151 (CHLA) between May 7 to November 21, 2020 for clinical testing for various indications  
152 including hospital admissions both related and unrelated to COVID-19, asymptomatic  
153 pre-procedural screening, evaluation of COVID-19 related and unrelated symptoms,  
154 and after a high-risk exposure to someone with confirmed SARS-CoV-2 infection. Data  
155 for demographics, clinical course and management were obtained from the electronic  
156 medical record (EMR). Disease severity was categorized using Centers for Disease  
157 Control and Prevention's classification as previously described.<sup>11</sup> The study was  
158 approved by the CHLA Institutional Review Board (CHLA-16-00429).

159

#### 160 **Detection of SARS-CoV-2 RNA**

161 Nasopharyngeal swabs or combined oropharyngeal and nares swabs were sent to the  
162 Clinical Virology Laboratory at CHLA for testing. The molecular assays used were the  
163 CDC 2019-Novel Coronavirus Real-Time RT-PCR assay, the Taqpath COVID-19 RT-  
164 PCR assay (Thermo Fisher, Walham, MA), the Xpert Xpress SARS-CoV-2 assay  
165 (Cepheid, Sunnyvale, CA), and the Simplexa COVID-19 assay (Diasorin Molecular,  
166 Cypress, CA). Total nucleic acid was extracted according to manufacturer's instructions  
167 as outlined in the respective Emergency Use Authorization.<sup>11-14</sup> Viral loads (copies/mL)  
168 were calculated based on a standard curve generated by testing samples with known  
169 viral copy numbers for each assay as previously described.<sup>11</sup>

170

## 171 **Viral culture**

172 Viral culture was performed using SARS-CoV-2-susceptible VeroE6TMPRSS2 cells<sup>15,16</sup>  
173 adapted from the VeroE6 cell line (ATCC CRL-1586) to express the TMPRSS2  
174 protease at levels approximately 10-fold higher than that found in the human lung. 150  
175  $\mu$ L of clinical specimen was used to inoculate one well of a 24 well plate of  
176 VeroE6TMPRSS2 cells as previously described.<sup>15,16</sup> After a 2-hour incubation at 37°C,  
177 the inoculum was removed and replaced with 0.5 ml infection media and the plates  
178 incubated at 37°C for 5 days. The plates were scored daily for cytopathic effect and  
179 supernatants harvested when >75% of the cells had detached. The presence of SARS-  
180 CoV-2 viruses in the harvested supernatants was then verified by quantitative RT-PCR  
181 using the CDC N1 and RNase P primer sets on RNA extracted with the viral RNA  
182 isolation kit (Qiagen, Germantown, MD).

183

## 184 **Quantitative Two-step strand-specific SARS-CoV-2 RT-PCR**

185 A two-step strand-specific SARS-CoV-2 RT-PCR assay targeting the *envelope* (E) gene  
186 was performed as previously described by Hogan et al. as a biomarker to predict  
187 presence of actively replicating virus.<sup>17</sup> In the first set of reactions, reverse transcription  
188 with strand-specific primers converts SARS-CoV-2 RNA to complementary DNA  
189 (cDNA). In the second step, the cDNA is amplified by real-time PCR in using the Rotor-  
190 Gene Q instrument (QIAGEN). A standard-curve to convert minus-strand Ct values to  
191 copies/ $\mu$ L was generated using *in vitro* transcribed minus-strand *E* gene RNA.

192

## 193 **Subgenomic SARS-CoV-2 RT-PCR**

194 One-step subgenomic (sg) SARS-CoV-2 RT-PCR utilizing a forward primer targeting  
195 the 5' leader sequence and reverse primer and probe complementary to *E* gene  
196 sequences was adapted from Wolfel et al. and combined in multiplex with the Hong  
197 Kong Orf1ab and Centers for Disease Control and Prevention RNase P primer/probe  
198 sets<sup>18,19</sup> as an additional biomarker for actively replicating virus. Real-time RT-PCR was  
199 performed using the Rotor-Gene Q instrument. A standard-curve to convert sgRNA Ct  
200 values to copies/ $\mu$ L was generated using *in vitro* transcribed plus-strand RNA encoding  
201 the leader and *E* gene sequences ( $\text{Log}_{10} \text{copies}/\mu\text{L} = -0.288 \cdot \text{Ct} + 11.351$ ).

202

## 203 **Measurement of anti-SARS-CoV-2 antibodies in serum**

204 IgG to the S1 domain of SARS-CoV-2 spike was measured from serum within 24 hours  
205 of collection with a commercial enzyme-linked immunosorbent assay (ELISA) kit  
206 (EUROIMMUN, Lubeck, Germany).<sup>20</sup> A ratio of sample to calibrator optical density of <

207 0.8 is considered negative,  $\geq 0.8$  to  $<1.1$  is considered borderline, and  $\geq 1.1$  is  
208 considered positive.

209

210 In addition, IgA, IgG and IgM to SARS-CoV-2 nucleocapsid (N) protein, spike S1, and  
211 receptor binding domain (RBD) and the competition ELISA procedure were measured  
212 as recently described by Röltgen et al.<sup>21</sup>

213

### 214 **Viral genome library construction and sequencing**

215 Whole-genome sequencing (WGS) libraries of viral cDNA were prepared as previously  
216 described using the CleanPlex SARS-CoV-2 Research and Surveillance NGS Panel  
217 (Paragon Genomics, Hayward, CA).<sup>11</sup> Libraries were then quantified and normalized to  
218 approximately 7nM and pooled to a final concentration of 4nM; libraries were denatured  
219 and diluted according to Illumina protocols and loaded on the MiSeq at 10pM. Paired-  
220 end and dual-indexed 2x150bp sequencing was done using Micro Kit v2 (300 Cycles).  
221 Libraries yielding average depth  $\geq 1000x$  were considered high quality and used for  
222 downstream analysis, and variant calling was performed for nucleotide positions with  
223  $\geq 100x$  coverage.

224

### 225 **Genome assembly and variant calling**

226 Coverage profiles, variant calls and consensus genomes were generated using the in-  
227 house software system LUBA (Lightweight Utilities for Bioinformatics Analysis).<sup>11</sup> Ion  
228 Torrent aligner TMAP (Thermo Fisher) was used to generate AmpliSeq BAMs.  
229 Sequencing of majority of clinical specimens by two alternate methods were also

230 pursued to validate Paragon variant calls (appendix p 1-3). Paragon and Twist  
231 nucleotide sequences were aligned with NovoAlign (Novocraft Technologies, Selengor,  
232 Malaysia) aligner. Ion Torrent aligner TMAP (Thermo Fisher) was used to generate  
233 AmpliSeq BAMs.

234

### 235 **Role of the funding source**

236 The funder had no role in study design, data collection, data analysis, data  
237 interpretation, or writing of the report. The corresponding author had full access to all  
238 the data in the study and had final responsibility for the decision to submit for  
239 publication.

240

### 241 **Results**

#### 242 Viral detection by RT-PCR and culture

243 Specimens from all three patients were collected and used to detect SARS-CoV-2 RNA  
244 over the course of 6 months. In addition to viral culture, we performed strand-specific  
245 and subgenomic RT-PCR to detect ongoing replication.<sup>4,17,18</sup> The viral load in patient 1  
246 was highest at day 0 and then gradually declined and was last reliably detected on day  
247 46 (Figure 2A). Culturable virus was only detected in the day 0 sample and subsequent  
248 cultures were negative. The SARS-CoV-2 minus strand and subgenomic RNA was only  
249 detected from the first sample taken on day 0 and not in any subsequent samples  
250 (Figure 2A).

251

252 The viral load in patient 2 remained consistent through day 172 despite two courses of  
253 Remdesivir and weekly administration of convalescent plasma. Consistent with these  
254 results, SARS-CoV-2 was recovered by viral culture for up to day 144. Viral cultures  
255 were not explored past 144 days from initial positive. Strikingly, the minus strand and  
256 subgenomic RNA was detected in nearly all of the samples from patient 2 and the Ct  
257 values trended with the corresponding viral load (Figure 2B).

258  
259 Patient 3 also maintained consistent viral loads through day 162 despite weak  
260 seroconversion on day 83, and finally tested negative on day 196 (Figure 2C). He  
261 demonstrated variable viral recovery with positive cultures from days 0, 22, and 139,  
262 and negative cultures from days 15, 67, and 162 which we believe reflects poor sample  
263 integrity or a transient reduction in infectious virus production given that subgenomic  
264 and minus strand RNA was readily detectable up through day 162.

265  
266 Antibody response

267 We assessed each patient's serological response profile using ELISAs to measure IgA,  
268 IgG, and IgM antibodies specific to the SARS-CoV-2 receptor binding domain (RBD),  
269 S1, and N proteins. Patient 1 had a strong IgA, IgG, and IgM response to all tested  
270 antigens at days 46 and 117, consistent with their more typical clinical course of  
271 infection and recovery, with viral RNA not reliably detected after day 46 (Figure 3A). In  
272 contrast, patient 2, who had culturable virus up to day 144 and positive viral RNA up to  
273 day 172, was more weakly IgG positive and was negative for IgA and IgM to all tested  
274 SARS-CoV-2 antigens from days 110-144 (Figure 3B). Importantly, paired sera

275 obtained from patient 2 before and after convalescent plasma infusion showed  
276 increased IgG levels after infusion which were rapidly waning. As this patient had B-cell  
277 aplasia following CAR T-cell therapy, his ability to mount an immune response was  
278 impaired. Patient 3 had detectable viral RNA at least up to day 162, and showed  
279 serological results spanning days 83-176 with a weakly positive IgG and unusually high  
280 levels of IgM for the RBD, S1, and Spike proteins, but negative N antibodies (Figure  
281 3C). Antibody levels were compared to four non-immunocompromised COVID-19  
282 patients, who showed the typical increase of anti-SARS-CoV-2 IgG, IgM, and IgA  
283 antibodies between one to two weeks after symptom onset. IgA and IgM antibody levels  
284 began to wane about 3 to 4 weeks after symptom onset, while IgG levels were more  
285 stable (Figure 3D).

286  
287 We also measured the ability of the patients' sera to interfere with the interaction  
288 between the RBD of the SARS-CoV-2 spike protein and the angiotensin-converting  
289 enzyme 2 (ACE2) receptor *in vitro* (Figure 3E). Sera from patient 1 from days 46 and  
290 117 achieved 100% blocking, whereas patient 2's sera only weakly blocked the ACE2-  
291 RBD interaction on day 123 post-infusion and the other timepoints failed to block the  
292 interaction. Samples from patient 3 from days 83, 141, and 176 also showed poor  
293 blocking activity (Figure 3E). Plasma samples from the four control patients showed  
294 varying degrees of RBD-ACE2 blocking activity. In a previous study higher RBD-ACE2  
295 blocking percentages were correlated with higher anti-RBD antibody levels<sup>21</sup> The  
296 antibody results were overall consistent with what we observed from the blocking assay,

297 with the strongest immune response in patient 1, least effective response in patient 2,  
298 and a weak response in patient 3.

299

### 300 Genomic sequencing analysis

301 Specimens from patient 1 showed only a single major allele variant difference between  
302 days 0 and 27. Decreasing viral load precluded sequencing of specimens from later  
303 timepoints. Patients 2 and 3 demonstrated an increase in intra-host viral diversity over  
304 time in variants of both high (major) and low (minor) allele frequencies across the viral  
305 genome (Figure 4). In patient 2, 3 major allele variants emerged between days 0 and 40  
306 with an additional 4 major and 7 minor allele variants by day 144. In patient 3, 13 major  
307 and 8 minor allele variants emerged by day 162. Virus clade predictions did not change  
308 across the specimens from each patient (patients 1 and 3: clade 20C and patient 2:  
309 clade 20A), providing further support that these patients were continuously infected  
310 rather than reinfected. Of particular note was the emergence of several spike gene  
311 mutations including 3 inframe deletions at residues S:Δ141-143, S:Δ145, and S:Δ141-  
312 144, a deletion-insertion at S:Δ211-212, and several nonsynonymous mutations  
313 including N440K, V483A, and E484Q at residues that have independently mutated in  
314 other lineages (Figure 4, appendix p 6-12). Sequencing of additional library  
315 preparations by two alternate methods confirmed the variant calls (appendix p 1-3).

316

### 317 **Discussion**

318 We report two pediatric and one young adult patient with B-cell ALL with remarkably  
319 different courses of SARS-CoV-2 infection. Patient 1 had milder symptoms with rapidly

320 declining and nonviable virus and serological evidence of a robust immune response  
321 that is representative of a typical COVID-19 clinical course.<sup>1</sup> By contrast, patients 2 and  
322 3 experienced more severe COVID-19 characterized by serological evidence of a  
323 weaker immune response with evidence of prolonged infectious virus shedding and  
324 mutation accumulation demonstrating emergence of potential escape mutations.

325  
326 The infection control implications make it critically important to closely monitor  
327 immunocompromised patients who are persistently positive by SARS-CoV-2 RT-PCR  
328 and to determine whether or not the virus is actively replicating for a prolonged period of  
329 time. Using RT-PCR to detect subgenomic and negative-strand replication  
330 intermediates, we were able to identify ongoing replication throughout the samples from  
331 patient 2 (up to 144 days) and patient 3 (up to 162 days). It is notable that subgenomic  
332 RNA was readily detected for this length of time given that it is rarely detected past 8  
333 days.<sup>4,5,18</sup> Overall the detection of viral intermediates correlated very well with the viral  
334 culture data, suggesting these may serve an expeditious molecular surrogate for  
335 infectivity. Viral culture was intermittently positive up to day 139 in patient 3. As culturing  
336 methods are limited by sample quality and lower sensitivity compared to molecular  
337 methods, it is more likely that the consistently positive results by subgenomic and  
338 negative-strand RT-PCR accurately represented continued replication within patient 3.

339  
340 There has been considerable interest in the rapidly spreading SARS-CoV-2 B.1.1.7  
341 variant due to its potential increased transmissibility. Relative to the SARS-CoV-2  
342 reference sequence, B.1.1.7 has acquired 17 mutations, 8 of which are in the spike

343 gene. There is concern that such a divergent variant could have emerged from long-  
344 term replication within an immunocompromised host, especially with the lack of closely  
345 related viral isolates.<sup>9</sup> Although we did not find these mutations in our patients, we did  
346 observe mutations in several regions within the spike gene. A V70P mutation appeared  
347 at day 162 in patient 3, overlapping the region where a S:Δ69-70del in the B.1.1.7  
348 variant may enhance infectivity.<sup>22</sup> Several other observed mutations mapped to  
349 important residues in the spike gene. We observed emergence of a S:Δ141-144 and  
350 S:Δ145 deletion in patient 2 and a S:Δ141-143 deletion in patient 3. Similar mutations in  
351 this region of the spike gene have been found to abolish the binding of the anti-spike  
352 protein 4a8 blocking/neutralizing monoclonal antibody (Figure 3, Tables S3-4).<sup>7,23</sup>  
353 Additionally, in patient 3, N440K within the spike RBD emerged with an allele frequency  
354 of 0.51 on day 162 (Figure 3, Table S4). This variant was also found by another group  
355 to confer antibody escape.<sup>24</sup> This mutation is adjacent to the position of a N439K variant  
356 of interest currently circulating in several lineages in Europe, which may enhance affinity  
357 of the binding of the spike protein to the ACE2 receptor and influences binding of  
358 monoclonal antibodies.<sup>25</sup> At day 139 the sequenced specimen from patient 3 also had  
359 mutations at V483A and E484Q within the RBD. These residues were similarly  
360 associated with *in vitro* antibody binding and escape, and there has been interest in  
361 another mutation at the same position, E484K, which has emerged in the S.501Y.V2  
362 lineage in South Africa (Figure 3, Table S4).<sup>24,26-28</sup> Similar mutations at these positions  
363 (N440D, E484A, and E484K) have independently arisen within other persistently  
364 infected, immunocompromised patients.<sup>5,7</sup>  
365

366 Analysis of patient antibody responses was performed to aid in understanding the  
367 persistent detection of SARS-CoV-2. Patient 1 was associated with very limited  
368 detection of active replication and had high levels of ACE2-RBD blocking antibodies, a  
369 surrogate measure of potential viral neutralizing antibodies *in vivo*. Patients 2 and 3 by  
370 contrast both had poor antibody responses, associated with evidence of prolonged  
371 infectivity. In immunocompetent patients, IgM, IgG, and IgA antibodies are generally  
372 detectable by day 20 post symptom onset.<sup>21</sup> Patient 3 had an atypical persistence of  
373 high IgM levels on days 83, 141, and 176 without evidence of evolution to IgG or IgA,  
374 suggestive of an impaired immune response perhaps related to his partially  
375 immunocompromised state. It is unlikely that the detection of IgM in this patient is  
376 related to infection with a new viral strain as the majority of the mutations that emerged  
377 in patient 3 are rarely found in the general population (Table S4). In general, all three  
378 patients had higher levels of antibodies targeting RBD and S1 compared to N, and this  
379 pattern has been previously observed in patients with milder illness compared to  
380 patients who died or were admitted to intensive care units.<sup>21</sup> However, compared to  
381 patients 1 and 2, patient 3 completely lacked antibodies to the N protein (Figure 3C). It  
382 is possible that the spike-focused immune response, which weakly blocked ACE2, led  
383 to the emergence of escape mutants. There were more mutations in the spike gene,  
384 particularly in the RBD region, in patient 3 compared to patient 2 and many of these  
385 emerged on day 139 or 162, a time period where his antibody levels were rising. Patient  
386 2 was treated with two courses of remdesivir and several infusions of convalescent  
387 plasma, however antibody levels waned rapidly after each infusion, possibly due to  
388 redistribution in the body or partial consumption and clearance. These treatments failed

389 to control viral replication and did not apparently lead to as many mutations with the  
390 potential for immune escape as observed in patient 3. We note that anti-SARS-CoV-2  
391 antibody levels start to decrease as soon as one month after symptom onset in some  
392 previously healthy COVID-19 patients, therefore it is possible that our measurements at  
393 later time points may underestimate the peak antibody levels achieved by patients 2  
394 and 3 throughout their clinical course.<sup>21</sup>

395  
396 Our work demonstrates that immunocompromised pediatric and young adult patients  
397 are susceptible to prolonged viral infections with prolonged infectious virus shedding  
398 and mutation accumulation. The patients we report are immunocompromised to varying  
399 degrees, and support a potential correlation between host immune response and the  
400 emergence of viral variants, some of which may have the potential to escape antibody  
401 neutralization. One of the limitations of a small case series is the generalizability of  
402 findings and more work is needed to better understand the many host factors that can  
403 influence viral clearance and mutation within these patients. However, we conclude that  
404 the observed expanded intra-host heterogeneity of viral isolates from pediatric and  
405 young adult patients with suppressed immunity and correspondingly prolonged infection  
406 raises the possibility of emergence of variants with the potential to evade immune  
407 responses elicited during the course of infection or induced by vaccine. This possibility  
408 warrants further study and, in the meantime, serious consideration of extended infection  
409 control precautions and genomic monitoring in this patient population.

410

411 **Acknowledgments**

412 The authors thank the ATUM Bio team for optimization, production, and sharing of  
413 antigens used in this study. We would like to acknowledge NCBI, GISAID, and  
414 Nextstrain for providing valuable resources for SARS-CoV-2 genomics. We thank the  
415 National Institute of Infectious Diseases, Japan, for providing VeroE6TMPRSS2 cells.

416

#### 417 **Conflict of Interest**

418 S.D.B. has consulted for Regeneron, Sanofi, and Novartis on topics unrelated to this  
419 study. S.D.B., and K.R. have filed provisional patent applications related to serological  
420 tests for SARS-CoV-2 antibodies. All other authors have no competing interests.

421

#### 422 **References**

- 423 1 Sethuraman N, Jeremiah SS, Ryo A. Interpreting Diagnostic Tests for SARS-CoV-2.  
424 *JAMA* 2020; **323**: 2249.
- 425 2 CDC. COVID-19 and Your Health. Centers for Disease Control and Prevention.  
426 2020; published online Feb 11. <https://www.cdc.gov/coronavirus/2019-ncov/if-you-are-sick/quarantine.html> (accessed Dec 27, 2020).  
427
- 428 3 Walsh KA, Spillane S, Comber L, *et al.* The duration of infectiousness of individuals  
429 infected with SARS-CoV-2. *Journal of Infection* 2020; **0**.  
430 DOI:10.1016/j.jinf.2020.10.009.
- 431 4 Perera RAPM, Tso E, Tsang OTY, *et al.* SARS-CoV-2 Virus Culture and  
432 Subgenomic RNA for Respiratory Specimens from Patients with Mild Coronavirus  
433 Disease - Volume 26, Number 11—November 2020 - Emerging Infectious Diseases  
434 journal - CDC. DOI:10.3201/eid2611.203219.
- 435 5 Avanzato VA, Matson MJ, Seifert SN, *et al.* Case Study: Prolonged infectious SARS-  
436 CoV-2 shedding from an asymptomatic immunocompromised cancer patient. *Cell*  
437 2020; published online Nov 4. DOI:10.1016/j.cell.2020.10.049.
- 438 6 Baang JH, Smith C, Mirabelli C, *et al.* Prolonged Severe Acute Respiratory  
439 Syndrome Coronavirus 2 Replication in an Immunocompromised Patient. *J Infect*  
440 *Dis* DOI:10.1093/infdis/jiaa666.

- 441 7 Choi B, Choudhary MC, Regan J, *et al.* Persistence and Evolution of SARS-CoV-2 in  
442 an Immunocompromised Host. *New England Journal of Medicine* 2020; **0**: null.
- 443 8 Aydillo T, Gonzalez-Reiche AS, Aslam S, *et al.* Shedding of Viable SARS-CoV-2  
444 after Immunosuppressive Therapy for Cancer. *New England Journal of Medicine*  
445 2020; **0**: null.
- 446 9 Rambaut A, Loman N, Pybus O, *et al.* Preliminary genomic characterisation of an  
447 emergent SARS-CoV-2 lineage in the UK defined by a novel set of spike mutations.  
448 COVID-19 Genomics Consortium UK, 2020 [https://virological.org/t/preliminary-  
449 genomic-characterisation-of-an-emergent-sars-cov-2-lineage-in-the-uk-defined-by-a-  
450 novel-set-of-spike-mutations/563](https://virological.org/t/preliminary-genomic-characterisation-of-an-emergent-sars-cov-2-lineage-in-the-uk-defined-by-a-novel-set-of-spike-mutations/563) (accessed Dec 21, 2020).
- 451 10 Lineage-specific growth of SARS-CoV-2 B.1.1.7 during the English national  
452 lockdown. *Virological*. 2020; published online Dec 30. [https://virological.org/t/lineage-  
453 specific-growth-of-sars-cov-2-b-1-1-7-during-the-english-national-lockdown/575/1](https://virological.org/t/lineage-specific-growth-of-sars-cov-2-b-1-1-7-during-the-english-national-lockdown/575/1)  
454 (accessed Dec 31, 2020).
- 455 11 Pandey U, Yee R, Shen L, *et al.* High Prevalence of SARS-CoV-2 Genetic Variation  
456 and D614G Mutation in Pediatric Patients with COVID-19. *Open Forum Infect Dis*  
457 DOI:10.1093/ofid/ofaa551.
- 458 12 appliedbiosystems. TaqPath COVID-19 Combi Kit and TaqPath COVID-19 Combo  
459 Kit Advanced Instructions for Use. 2020; published online Nov 20.  
460 <https://www.fda.gov/media/136112/download> (accessed Dec 13, 2020).
- 461 13 DiaSorin Molecular. Simplexa COVID-19 Direct. 2020; published online May 28.  
462 <https://www.fda.gov/media/136286/download>.
- 463 14 Cepheid. Xpert Xpress SARS-CoV-2 Instructions for Use. 2020; published online  
464 Sept. <https://www.fda.gov/media/136314/download> (accessed Dec 13, 2020).
- 465 15 Gniazdowski V, Morris CP, Wohl S, *et al.* Repeat COVID-19 Molecular Testing:  
466 Correlation of SARS-CoV-2 Culture with Molecular Assays and Cycle Thresholds.  
467 *Clin Infect Dis* 2020; published online Oct 27. DOI:10.1093/cid/ciaa1616.
- 468 16 Pekosz A, Cooper CK, Parvu V, *et al.* Antigen-based testing but not real-time PCR  
469 correlates with SARS-CoV-2 virus culture. *medRxiv* 2020; : 2020.10.02.20205708.
- 470 17 Hogan CA, Huang C, MK S, *et al.* Strand-specific reverse transcription PCR for  
471 detection of replicating SARS-CoV-2. *Emerging Infectious Diseases* 2021; published  
472 online Feb. DOI:<https://doi.org/10.3201/eid2702.204168>.
- 473 18 Wölfel R, Corman VM, Guggemos W, *et al.* Virological assessment of hospitalized  
474 patients with COVID-2019. *Nature* 2020; **581**: 465–9.

- 475 19 Chu DKW, Pan Y, Cheng SMS, *et al.* Molecular Diagnosis of a Novel Coronavirus  
476 (2019-nCoV) Causing an Outbreak of Pneumonia. *Clin Chem* 2020; published online  
477 Jan 31. DOI:10.1093/clinchem/hvaa029.
- 478 20 Tilley K, Ayvazyan V, Martinez L, *et al.* A Cross-Sectional Study Examining the  
479 Seroprevalence of Severe Acute Respiratory Syndrome Coronavirus 2 Antibodies in  
480 a University Student Population. *J Adolesc Health* 2020; **67**: 763–8.
- 481 21 Röltgen K, Powell AE, Wirz OF, *et al.* Defining the features and duration of antibody  
482 responses to SARS-CoV-2 infection associated with disease severity and outcome.  
483 *Science Immunology* 2020; **5**. DOI:10.1126/sciimmunol.abe0240.
- 484 22 Recurrent emergence and transmission of a SARS-CoV-2 Spike deletion  $\Delta$ H69/V70  
485 | bioRxiv. <https://www.biorxiv.org/content/10.1101/2020.12.14.422555v3> (accessed  
486 Dec 26, 2020).
- 487 23 McCarthy KR, Rennick LJ, Nambulli S, *et al.* Natural deletions in the SARS-CoV-2  
488 spike glycoprotein drive antibody escape. *bioRxiv* 2020; : 2020.11.19.389916.
- 489 24 Weisblum Y, Schmidt F, Zhang F, *et al.* Escape from neutralizing antibodies by  
490 SARS-CoV-2 spike protein variants. *eLife* 2020; **9**: e61312.
- 491 25 Thomson EC, Rosen LE, Shepherd JG, *et al.* The circulating SARS-CoV-2 spike  
492 variant N439K maintains fitness while evading antibody-mediated immunity.  
493 *Microbiology*, 2020 DOI:10.1101/2020.11.04.355842.
- 494 26 Liu Z, VanBlargan LA, Rothlauf PW, *et al.* Landscape analysis of escape variants  
495 identifies SARS-CoV-2 spike mutations that attenuate monoclonal and serum  
496 antibody neutralization. *bioRxiv* 2020; : 2020.11.06.372037.
- 497 27 Andreano E, Piccini G, Licastro D, *et al.* SARS-CoV-2 escape in vitro from a highly  
498 neutralizing COVID-19 convalescent plasma. *bioRxiv* 2020; : 2020.12.28.424451.
- 499 28 Greaney AJ, Starr TN, Gilchuk P, *et al.* Complete Mapping of Mutations to the  
500 SARS-CoV-2 Spike Receptor-Binding Domain that Escape Antibody Recognition.  
501 *Cell Host & Microbe* 2021; **29**: 44-57.e9.

502

503

504

505

506

507

508 **Research in context**

509 *Evidence before this study*

510 There has been substantial interest in the phenomenon of prolonged shedding of  
511 SARS-CoV-2. Although an increasing number of case reports have described the  
512 course of disease in immunocompromised individuals, definitive evidence for prolonged  
513 active replication with infectious virus and corresponding immunological data has been  
514 scarce. We searched PubMed, bioRxiv, and medrxiv for these reports using the terms  
515 “immunocompromised,” “immunosuppressed,” “SARS-CoV-2,” “replication,” “shedding,”  
516 and “infectivity” for relevant articles published up until December 26, 2020. We found  
517 four articles that have utilized longitudinal sequencing, detection of subgenomic RNA,  
518 and/or viral culture to demonstrate ongoing infectivity in immunocompromised adults.

519

520 *Added value of this study*

521 Our study presents a more complete picture of the spectrum of prolonged infection for  
522 up to 162 days, which is the longest reported to-date, in three immunocompromised  
523 patients using viral culture, detection of both subgenomic and single-stranded RNA,  
524 whole-genome sequencing, and characterization of host serological responses.  
525 Secondly, this is the first report, to our knowledge, characterizing prolonged infection in  
526 pediatric and young adult patients. Thirdly, we demonstrated the clear presence of intra-  
527 host viral heterogeneity as evidence of ongoing viral evolution within the hosts. We note  
528 two of our patients acquired several mutations in the gene encoding the spike protein at  
529 specific residues that may be important for antibody binding. Finally, we present a

530 potential correlation between the host immune response and the emergence of  
531 mutations in the spike gene.

532

533 *Implications of all the available evidence*

534 Given recent interest in the emergence of a potentially more transmissible variant of  
535 SARS-CoV-2, there is a need to better understand the dynamics of within-host  
536 accumulation of mutations in immunocompromised hosts, whether or not they remain  
537 infectious, if these mutations could mediate immune escape, and what kind of  
538 immunological selection pressures may drive such mutations. Altogether, these findings  
539 have important public health implications for infection control precautions and  
540 management in this patient population.

541

542

543

544

545

546

547

548

549

550

551

552

553 **Figure Legends**

554 **Figure 1. Clinical timeline of symptoms, hospital admissions, and treatment.**

555 Timelines for patient 1 (A), patient 2 (B), and patient 3 (C) are labelled by date from  
556 initial positive RT-PCR (day 0). Colored bars indicate time periods where patients were  
557 symptomatic, required supplementary oxygen, or received treatment (Remdesivir or  
558 convalescent plasma). The phases of chemotherapy are also shown.

559

560 **Figure 2. Viral load by routine, negative-strand, and subgenomic RT-PCR.** Time

561 course of viral load from nasopharyngeal or combined nares/oropharyngeal swabs  
562 collected from each patient. Viral culture results are indicated in pink. Corresponding  
563 serum anti-SARS-CoV-2 IgG values are plotted in blue. For patient 2, IgG was  
564 measured before and after administration of convalescent plasma at the indicated  
565 timepoints.

566

567 **Figure 3. Anti-SARS-CoV-2 antibody responses in three immunocompromised**  
568 **pediatric and young adult patients.**

569 Serum samples from two immunocompromised children (A, C) and one young adult (B)  
570 were collected up to 176 days after initial positive SARS-CoV-2 PCR test. Plasma  
571 samples from four non-immunocompromised COVID-19 patients were analyzed for  
572 comparison (D). Antibodies specific for SARS-CoV-2 Spike RBD (top row), S1 subunit  
573 (second row), and N protein (third row) were measured using ELISA at 1:100  
574 serum/plasma dilution. RBD-ACE2 blocking activity was assessed in a competition  
575 ELISA and is shown as percentage of blocking (E). The cutoff for seropositivity was

576 defined as the mean absorbance + 3 SD of 94 pre-pandemic plasma samples in each  
577 assay (A, B, C, D). Color coding for isotypes: IgG (blue), IgM (green), IgA (red). Dotted  
578 lines depict the cutoff for seroconversion for the different isotypes in each assay.  
579 Individual donors were shown with different symbols (D). \* indicates timepoints of  
580 convalescent plasma infusion in patient 2.

581

582 **Figure 4. Accumulation of SARS-CoV-2 variants in three persistently positive**

583 **pediatric and young adult patients with hematologic malignancies.** Each row

584 represents viral culture, strand-specific RT-PCR (ssRT-PCR), subgenomic RT-PCR

585 (sgRT-PCR) and sequencing from longitudinally derived specimens numbered by days

586 from initial positive test (day 0). Boxes represent distinct variants, and shading reflects

587 variant allele frequency (cutoff = 0.25). Corresponding genes are labeled in top row and

588 colored to represent variant annotation (see legend). Specimens from two patients

589 demonstrate progressive accumulation of multiple variants and variants of lower allele

590 frequencies (Patient 2, difference of 7 major allele variants between days 0 and 144;

591 Patient 3, difference of 13 major allele variants between days 0 and 162). In addition to

592 point mutations, four different inframe deletions were observed to develop in the S gene

593 in Patient 2 and Patient 3. Several variants (both major and minor alleles) reverted at

594 later timepoints.

595

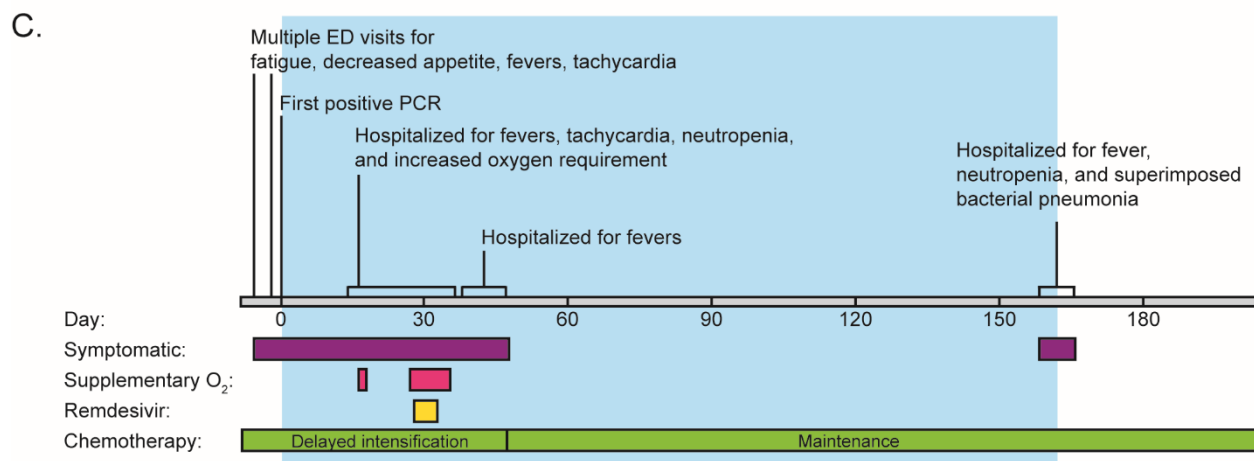
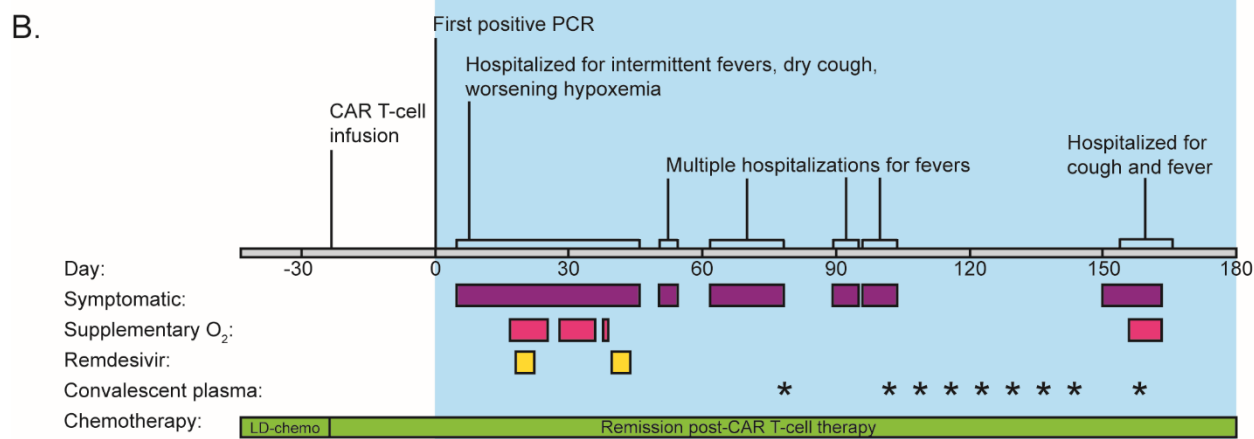
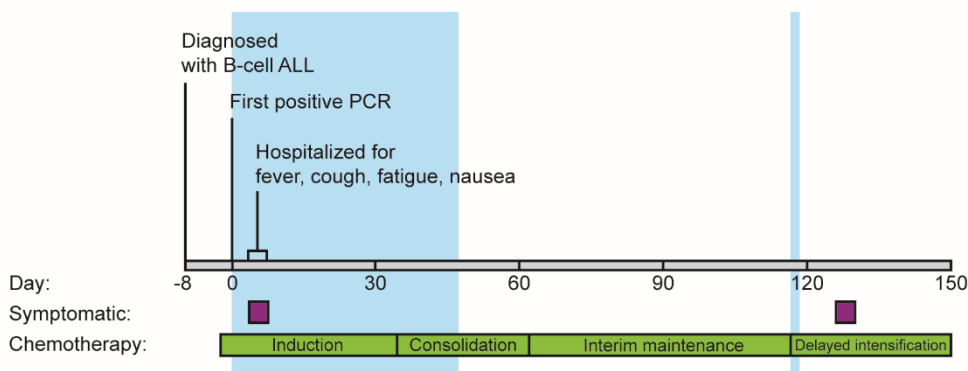
596 UTR, untranslated region; S, spike; E, envelope; M, matrix; N, nucleocapsid

597

598

599 **Figure 1.**  
600

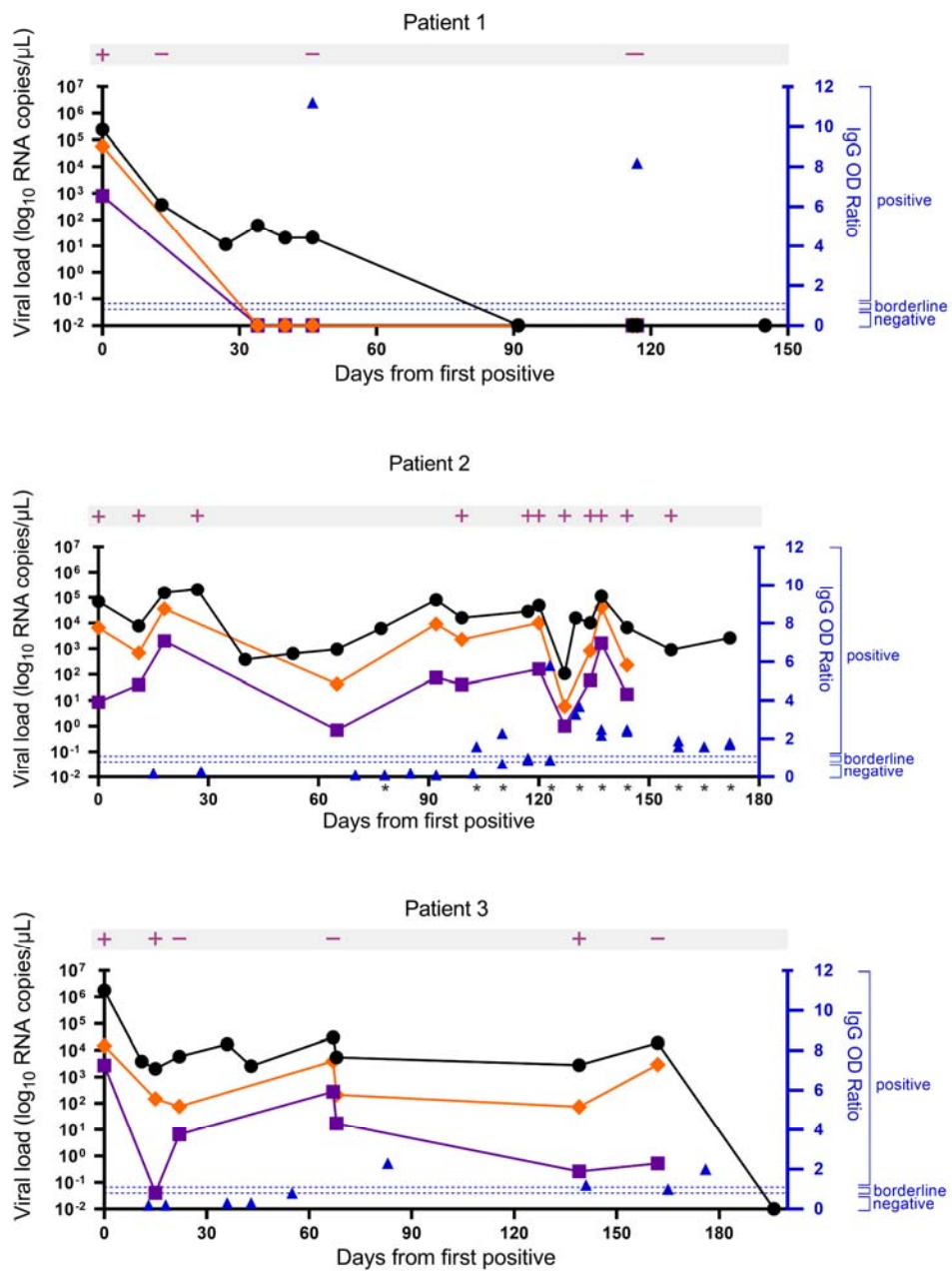
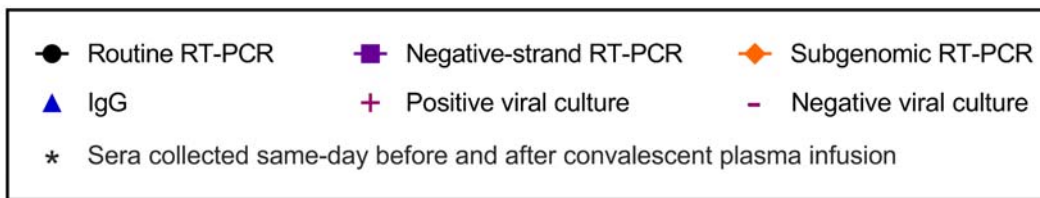
A.  Shaded regions represent RT-PCR positivity



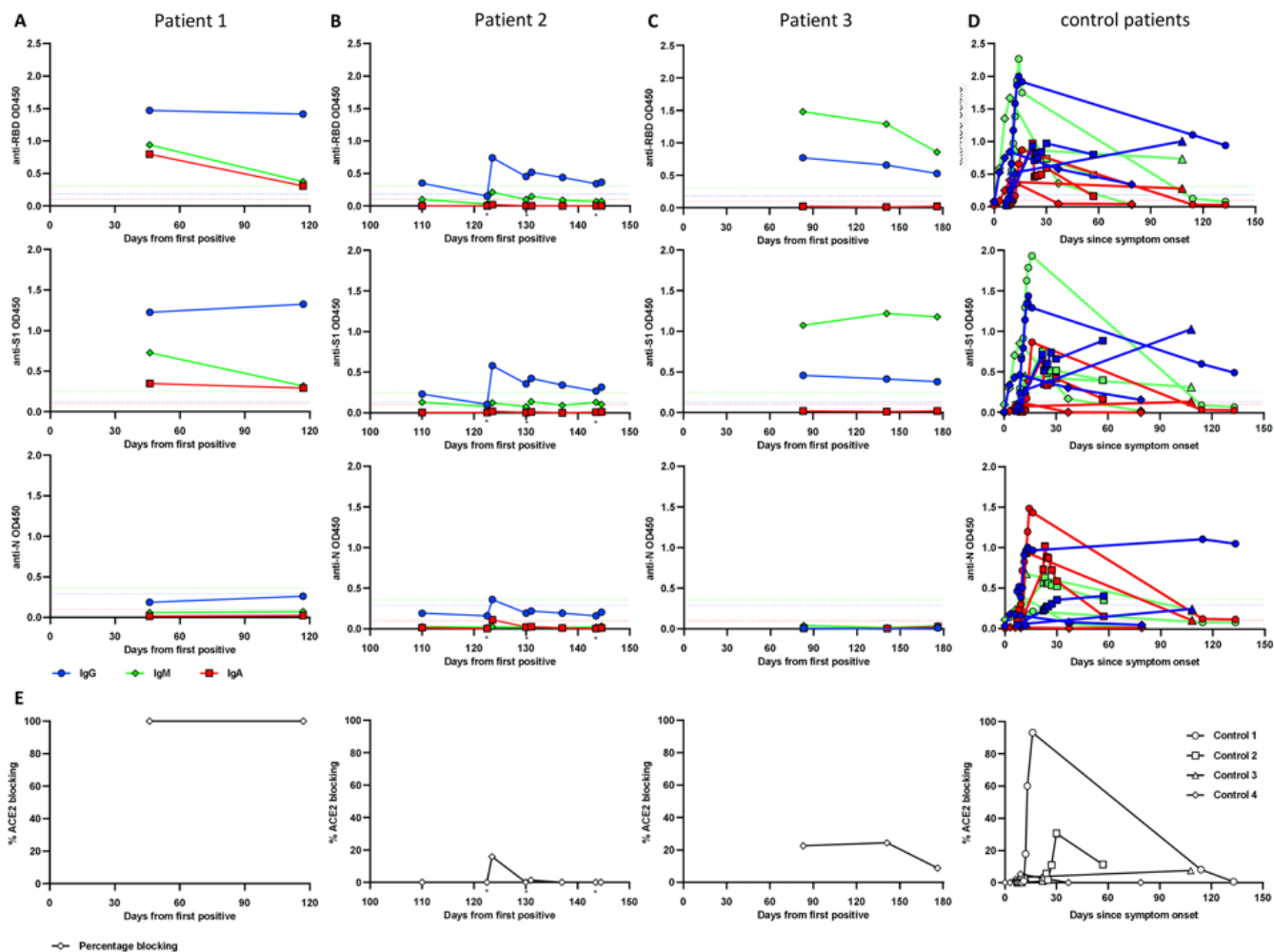
601

602

603 **Figure 2.**



605 **Figure 3.**



606

607

608

609

610

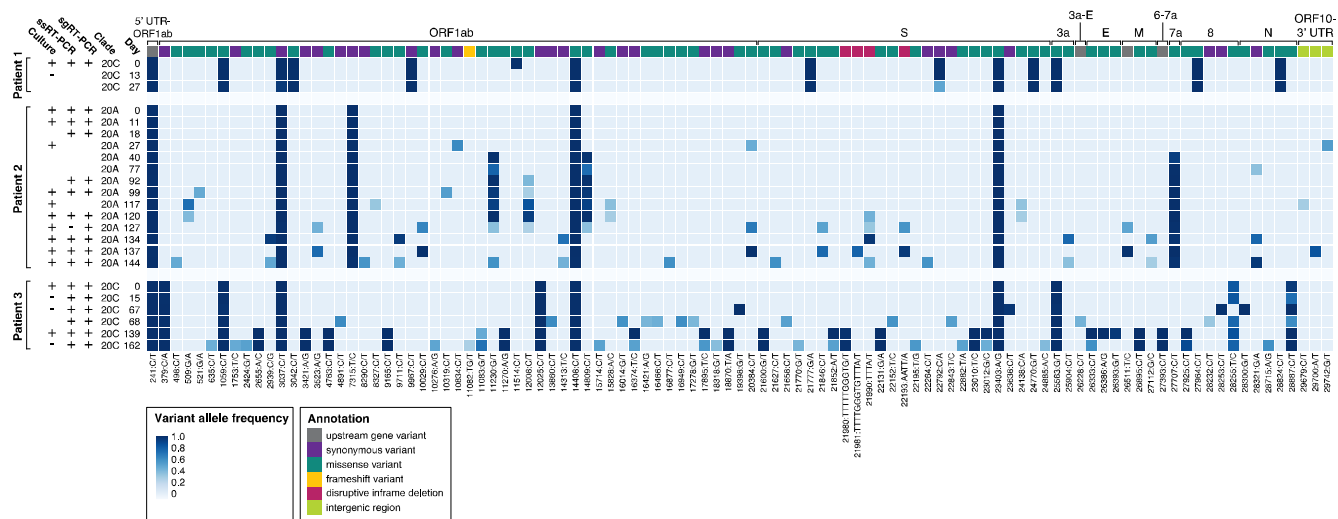
611

612

613

614

615 **Figure 4.**



616

617

618 **Table 1.** Demographic, oncological, and clinical characteristics of study patients.

	Patient 1	Patient 2	Patient 3
<b>Demographic characteristics</b>			
Age range (years)	0-5	20-25	0-5
Sex	Female	Male	Male
Body Mass Index	16.6 kg/m <sup>2</sup>	27 kg/m <sup>2</sup>	16.3 kg/m <sup>2</sup>
<b>Oncological characteristics</b>			
Oncological diagnosis	SR B-ALL	HR B-ALL, refractory	HR B-ALL
Other coexisting medical conditions	None	Obstructive sleep apnea Hypothyroidism Intermittent Asthma	None
Oncological treatment	Chemotherapy	Lymphodepleting chemotherapy and CAR-T cell therapy	Chemotherapy
Phases of oncological treatment during viral shedding	-Induction -Consolidation -Interim maintenance -Delayed intensification	Post- CAR-T cell therapy	-Delayed intensification -Maintenance
Active immunosuppressive or immunomodulatory drugs?	SR B-ALL chemotherapy per COG AALL0932: Dexamethasone, vincristine, peg-asparaginase, methotrexate, 6-MP, doxorubicin	Cyclophosphamide and Fludarabine as lymphodepleting agents prior to CAR-T cell therapy	HR B-ALL chemotherapy per COG AALL0232: Cyclophosphamide, cytarabine, thioguanine, vincristine, dexamethasone, methotrexate, mercaptopurine
Chemotherapy	Yes (detailed above)	Yes (detailed above)	Yes (detailed above)
Corticosteroids	Yes (per chemotherapy protocol)	No	Yes (per chemotherapy protocol)
CAR-T therapy	No	Yes, Tisagenlecleucel	No
<b>Clinical, laboratory and imaging data</b>			
Days of PCR positivity	46 (inconclusive/positive again day 116-117)	165+ from time of report	162
Symptomatic at time of initial positivity	No	No	Yes
Symptomatic at any positive time point	Yes	Yes	Yes
<b>Symptoms</b>			
Fever	Yes	Yes	Yes
Malaise	Yes	Yes	Yes
Cough	Yes	Yes	Yes
Sore throat	Yes	No	Yes
Headache	No	No	No
Shortness of breath	No	Yes	Yes
Congestion/rhinorrhea	No	Yes	Yes
Vomiting	Yes	Yes	Yes
Abdominal pain	Yes	Yes	Yes
Anosmia and Ageusia	Unable to assess	Unable to assess	Unable to assess

Other infectious disease findings	No	- <i>Clostridioides difficile</i> diarrhea - <i>Staphylococcus hominis</i> bacteremia (day +7)	Superimposed bacterial pneumonia (day 162, improved with antibiotics)
Laboratory data at initial positivity	WBC: 2.14 K/ $\mu$ L ANC: 0.74 K/ $\mu$ L ALC: 1.36 K/ $\mu$ L	WBC: 2.30 K/ $\mu$ L ANC: 1.59 K/ $\mu$ L ALC: 0.42 K/ $\mu$ L	WBC: 0.65 K/ $\mu$ L ANC: 0.00 K/ $\mu$ L ALC: 0.56 K/ $\mu$ L
Lymphocyte subsets	Not done	Day +7 to +158 (multiple) CD3: 75-1000 cells/ $\mu$ L CD4: 31-314 cells/ $\mu$ L CD8: 52-747 cells/ $\mu$ L CD19: <1 cell/ $\mu$ L throughout	Day +13 CD3: 1204 cells/ $\mu$ L CD4: 194 cells/ $\mu$ L CD8: 987 cells/ $\mu$ L CD19: 1 cells/ $\mu$ L
Chest CT scan	Not done	Bilateral patchy ground glass opacities involving all lobes, predominantly peripherally in lower lobes (similar in all 3 CT scans on days +38, +73 and +116)	Persistent multifocal pneumonia and scattered areas of ground-glass opacities, with shifting opacities increased in some areas but improved in others (CT scans on days +22, +47, +96, +166)
<b>Treatment for COVID-19 infection</b>			
Oxygen supplementation	No	Yes, intermittent (maximal 10L per minute via facemask)	Yes (maximal 5L per minute via facemask)
COVID-19 related ICU admissions	No	Yes (5 days)	No
Mechanical ventilation	No	No	No
Remdesivir	No	Yes, two 5 day courses	Yes, one 5 day course
Convalescent plasma	No	Yes (measured as ratio serum to calibrator absorbance) Day 78: 4.3 Day 103: 9.1 Day 110: 8.6 Day 123: 8.3 Day 130: 7.5 Day 137: 4.6 Day 144: 1.4 Day 158: 4.1 Day 165: 3.4 Day 172: 1.53	No

619 SR, standard risk; HR, high risk; B-ALL, B-cell acute lymphocytic leukemia; CAR-T,  
620 chimeric antigen receptor T-cell therapy; COG, Children's Oncology Group; WBC, white  
621 blood cells; ANC, absolute neutrophil count; ALC, absolute lymphocyte count; CT,  
622 computerized tomography; ICU, intensive care unit  
623

624